

Close range photogrammetry and self-organizing map for automatic diagnosing diseases

Farshid Farnood Ahmadi¹

Received: 31 January 2015 / Accepted: 10 June 2015 / Published online: 24 June 2015
© The Natural Computing Applications Forum 2015

Abstract The output of close range photogrammetry is a finite set of 3D points which causes generating a discrete space. The dataset is a point cloud with no defined topology and structure. For diagnosing disease precisely using close range photogrammetry, specifically in an intelligent manner, it is necessary to reconstruct and parameterize a continuous and topology-definable surface from the measured points. Traditional methods for surface reconstruction such as interpolation and using approximation functions do not provide topological information and required details for shape analysis and disease diagnosis. According to SOM abilities for reconstruction of the space of measured points as a fully structured and topology-definable surface, in this research, a medical system has been designed and implemented by integration of SOM and close range photogrammetry. The research result shows that SOM is an effective tool for recognizing the pattern of measured points and generating a reference surface around affected areas. So, close range photogrammetry and SOM can be used to develop integrated systems as two complementary techniques for diagnosing diseases whose symptoms are visible or appear as deformations out of body and around the affected area.

Keywords Automatic diagnosing diseases · Medical photogrammetry · Self-organizing map

1 Introduction

Close range photogrammetry is a high-precision measurement technique for capturing 3D spatial data using two or more overlapped images [1]. Close range photogrammetry has been used in many medical applications as a measurement tool for diagnosing disease [2]. Some of these applications include: craniofacial mapping [3], human trunk and limb measurement [4], dental measurement [5], wound and bed sore measurement [6], and intelligent diagnosing disease [7]. In most of the applications, 3D coordinates of a limited number of points are determined using colinearity equations, and all measurements are carried out based on the points. The finite set of 3D points causes generating a discrete space which is suitable only for discrete data analysis. For diagnosing disease precisely using close range photogrammetry, specifically in an intelligent manner, it is necessary to reconstruct and parameterize a continuous surface from the measured 3D points. Generally, three methods have been used for reconstructing a continuous surface from 3D points. The methods include: using artificial neural network [8], interpolation [9–11], and using approximation functions [12, 13]. Each of the methods fits a good surface to measured points, and reconstruction process is carried out well, but these methods do not provide required details for shape analysis and disease diagnosis. For example, one of the common methods for modeling a surface based on 3D measured points is Triangulated Irregular Network (TIN). TIN is a vector-based representation of physical surfaces, made up of irregularly distributed nodes and lines with 3D coordinates (x , y , and z) that are arranged in a network of nonoverlapping triangles. TIN is only useful for representation of a 2.5D surface (a surface which is continuous, and all locations on the surface can have only one elevation, or z -value, per x and

✉ Farshid Farnood Ahmadi
farnood@tabrizu.ac.ir

¹ Department of Geomatics Engineering, Faculty of Civil Engineering, University of Tabriz, Tabriz, Iran

y coordinates). So, it cannot be used to represent an actual 3D surface which has multiple z -values for any given x and y locations. Another trouble about the reconstruction methods which is important for medical applications is caused by incorrect topological relations between sampled points. If measured points are not dens or uniform, wrong holes may appear on undesirable places over the surface [14]. Self-organizing map (SOM) is a type of artificial neural network which is training by unsupervised learning method to generate a low-dimensional representation of the space of the training samples. A self-organizing map uses a neighborhood function to preserve topological properties of the space [15]. So, SOM can be used for solving the problems in reconstruction and parameterization of surfaces around affected areas on the body.

According to the measurement capabilities of close range photogrammetry as a precise 3D spatial data acquisition technique and SOM abilities for reconstruction of the space of measured points around desired location on the body, the main idea in this research is to design and implement a medical system for automatic diagnosing diseases by integration of these techniques. The integrated system can be used for the diseases whose symptoms are visible or appear as deformations out of body and around the affected area. For evaluation of the system functionality, the system has been applied for automatic diagnosing foot deformity.

2 Background

2.1 Medical photogrammetry

The basis of close range photogrammetry is triangulation, whereby intersection of converging rays in space is used to determine the position of points in all three dimensions [1]. To do so, the orientation of cameras for each captured image is needed. The orientation parameters of cameras are calculated through resection process. To be able to run this process, at least 12 well-disturbed points on each image are needed. Some advantages of close range photogrammetry as a measurement technique are:

- It is a noncontact, noninvasive, and instantaneous technique (synchronized for all measurements)
- It offers high-accuracy and high-precision measurements
- It provides possibility of measuring any number of points on the object [16]
- It provides possibility of a fully automatic measurement [17]
- It uses optical images which are remotely taken, and has no side effect to the human organism [18].

According to the advantages and capabilities of the close range photogrammetry, nowadays, one of the special domains which it is applied is medicine. In this application, the subject of imaging is human and the method called Medical Photogrammetry. The aim of medical photogrammetry is to assist in health matters. It usually is used to diagnose a disease or monitor its effects. It is also applied to prevent diseases which are probable during sports and ergonomic studies [19].

2.2 Self-organizing map (SOM)

Self-organizing map is a type of artificial neural networks that uses a nonlinear projection from the high-dimensional space of input signals onto a low-dimensional space of neurons [20]. SOM uses a neighborhood function to preserve topological properties of the space. SOM can learn data modeling and classification without external supervision. So, training a SOM does not require target vectors. Another advantage of SOM is that although it is a type of artificial neural networks, it does not use complex activation functions and feed-forward/recurrent connections. Using SOM, all vectors containing sampled values participate in reconstruction and parameterization process.

A self-organizing map network consists of components called nodes or neurons. Associated with each node is a weight vector of the same dimension as the input data vectors and a position in the map space. The usual arrangement of nodes is a two-dimensional regular spacing in a hexagonal or triangular grid. Each of the nodes is fully connected to the input layer.

If the training data consist of vectors, V , of n dimensions (V_1, V_2, \dots, V_n), then each node will contain a corresponding weight vector, W , of n dimensions (W_1, W_2, \dots, W).

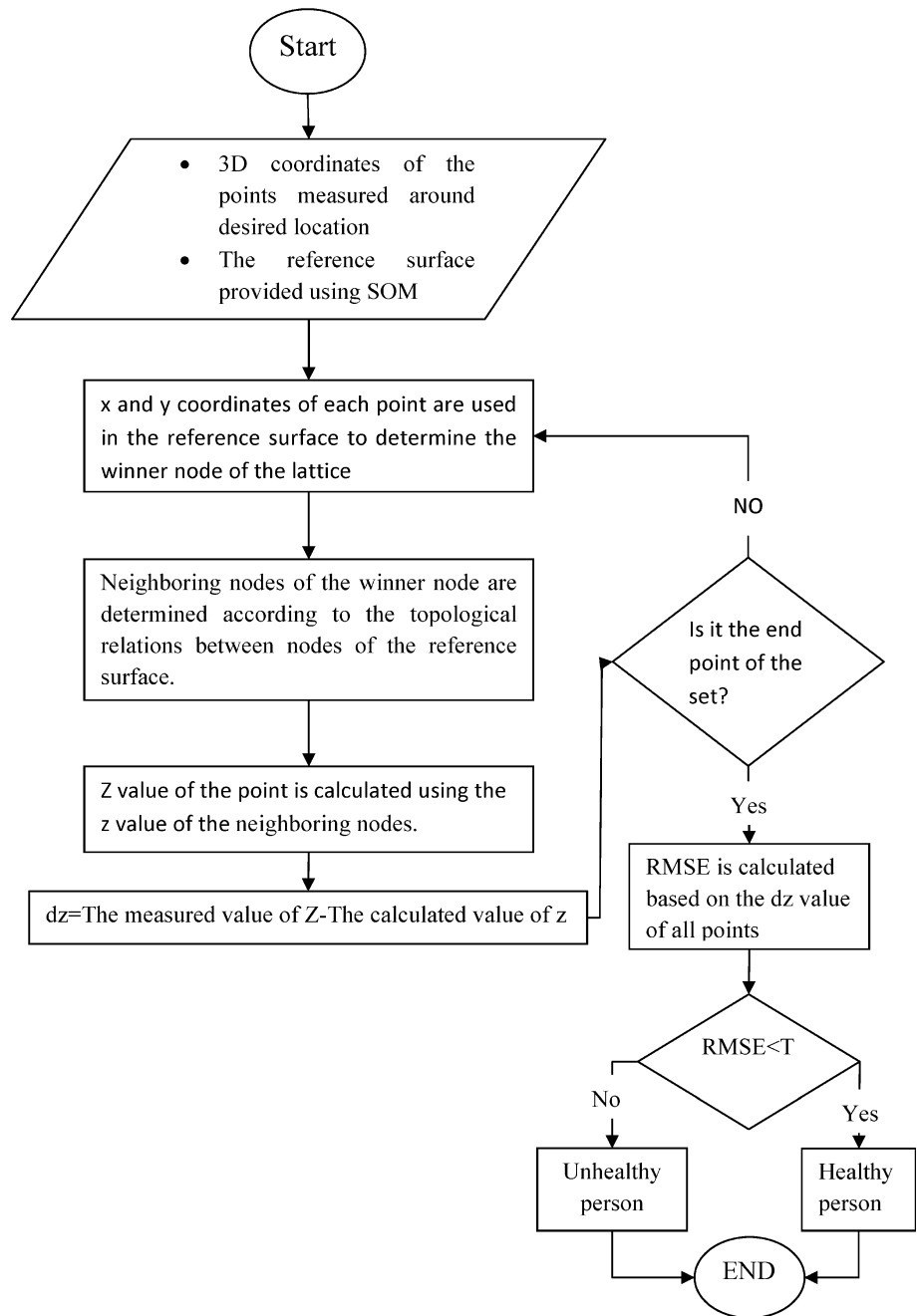
A SOM network does not need a target output to be specified. Instead, where the weights match the input vector that area of the network is optimized to more closely resemble the data for the class the input vector is a member of.

Prior to training, each weight must be initialized. Typically the weights will be set to small standardized random values.

To determine the best matching unit, one method is to iterate through all the nodes and calculate the Euclidean distance between each weight vector and the current input vector. The node with a weight vector closest to the input vector is tagged as the best matching unit (BMU). The Euclidean distance is given as:

$$\text{Distance} = \sqrt{\sum_{i=0}^{i=n} (V_i - W_i)^2} \quad (1)$$

Fig. 1 Flowchart of diagnosing process



where V is the current input vector and W is the node’s weight vector.

The next step is to calculate which of the other nodes are within the BMU’s neighborhood. It can be carried out by defining a radial distance and selecting the nodes which are within the distance. These nodes will have their weight vectors altered in the next step. The area of the neighborhood shrinks over time. This is accomplished by making the radius of the neighborhood shrink over time using dynamic functions such as exponential decay function:

$$\sigma(t) = \sigma_0 \exp\left(-\frac{t}{\lambda}\right) \quad t = 1, 2, 3, \dots \quad (2)$$

where σ_0 denotes the width of the lattice at time t_0 and λ denotes a time constant. t is the current time-step. The value of λ is dependent on σ and the number of iterations chosen for the algorithm to run. Each node within the BMU’s neighborhood (including the BMU) has its weight vector adjusted according to the following equation:

$$W(t + 1) = W(t) + LR(t)(V(t) - W(t)) \quad (3)$$

Fig. 2 System architecture

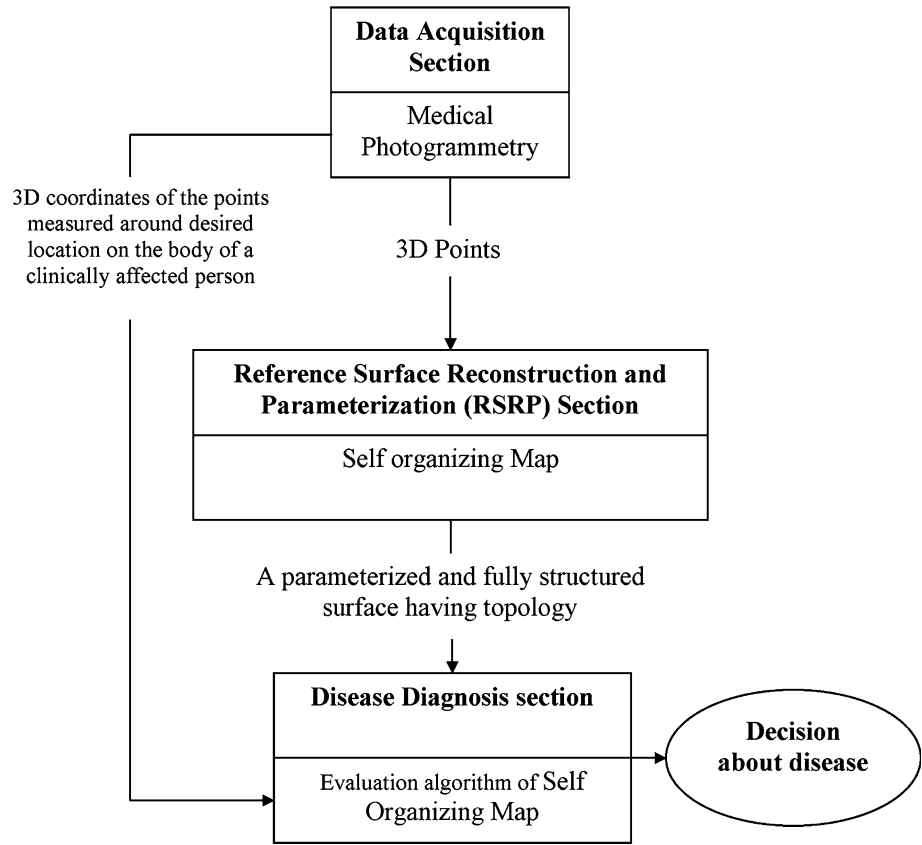
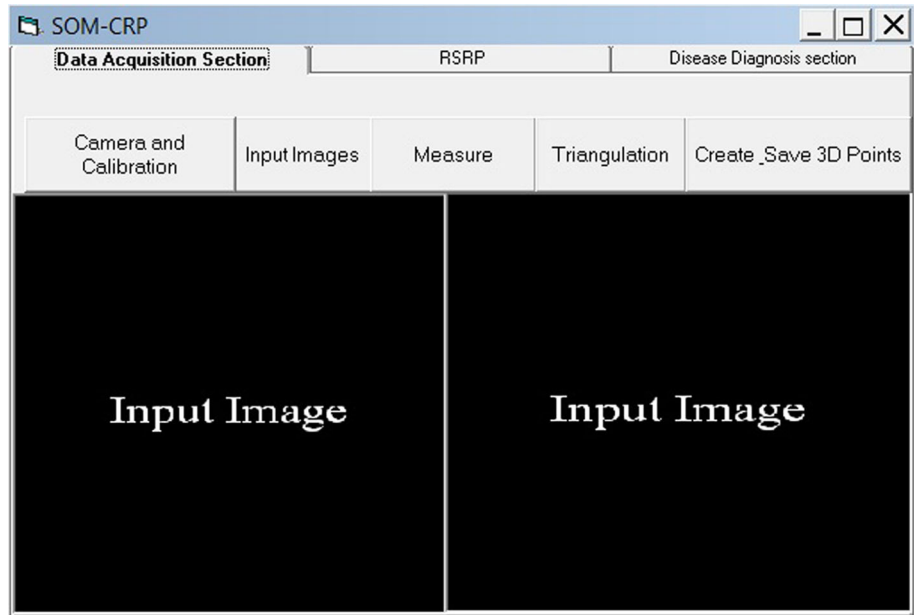


Fig. 3 User interface of the system



where t represents the time-step and LR is a small variable called the learning rate, which decreases with time. The decay of the learning rate is calculated for each iteration using the following equation:

$$LR(t) = LR_0 \exp\left(-\frac{t}{\lambda}\right) \quad t = 1, 2, 3, \dots \quad (4)$$

Not only the learning rate has to decay over time, but also the effect of learning should be proportional to the distance

Table 1 Camera specifications

Camera specifications	
Name	Canon
Model	SX230 HS
Focal length	5 mm
Format size	6.1976 × 4.6482

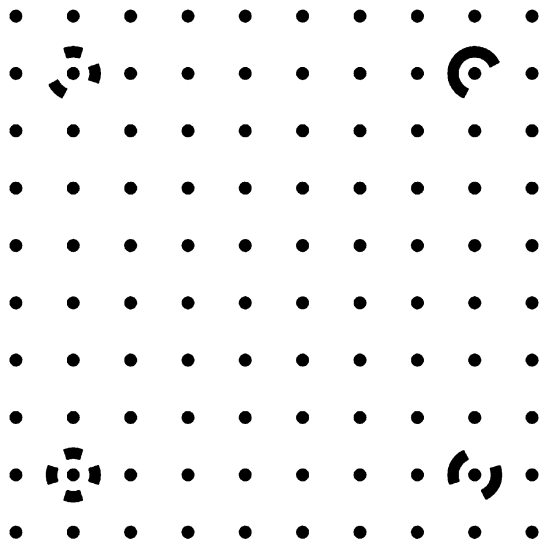


Fig. 4 Portable target sheet

Table 2 Result of camera calibration

Parameter	Value	Deviation
F—focal length	5.136117 mm	6.6e−004 mm
Xp—principal point x	3.006697 mm	7.3e−004 mm
Yp—principal point y	2.254488 mm	8.3e−004 mm
K1—radial distortion 1	1.162e−003	2.0e−005
K2—radial distortion 2	−7.816e−006	1.6e−006
K3—radial distortion 3	0.000e+000	−
P1—decentering distortion	1.461e−003	9.7e−006
P2—decentering distortion 2	−6.598e−004	1.1e−005

of a node from the BMU. Ideally, the amount of learning should fade over distance similar to the Gaussian decay. To achieve this, Eq. 3 can be developed as:

$$W(t + 1) = W(t) + \Theta(t)LR(t)(V(t) - W(t)) \tag{5}$$

$$\Theta(t) = \exp\left(-\frac{\text{Distance}^2}{2\sigma^2(t)}\right) t = 1, 2, 3, \dots \tag{6}$$

where Distance is the distance of a node from the BMU and σ is the width of the neighborhood function as calculated by Eq. 2. Additionally, please note that Θ also decays over

time [21]. After training process, each neuron will contain information about the vectors and neighborhood relations.

In this research, each of the vectors contains coordinates of a 3D point measured around desired location on the body using medical photogrammetry technique.

3 System architecture

The medical system designed in this research consists of three main sections. The sections are:

1. Data acquisition section for getting required data from the affected area
2. Reference surface reconstruction and parameterization (RSRP) section
3. Disease diagnosis section

3.1 Data acquisition section

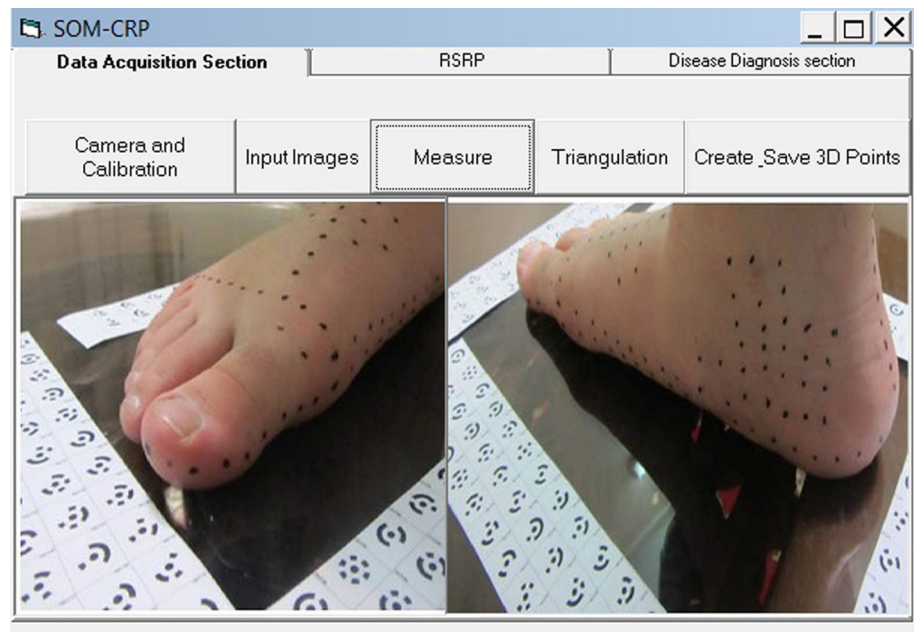
In order to choose an appropriate technique for implementation of the data acquisition section, four following factors should be considered:

- Using the system should be simple enough for nonexpert operators at clinical environments
- The system should be affordable
- The system should be safe for patients and has no side effect on human body
- The system should be capable of reconstructing 3D model with high accuracy and precision

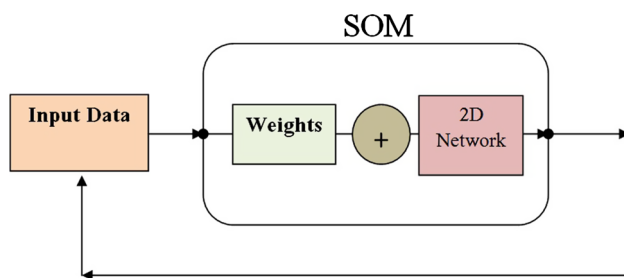
According to the advantages of close range photogrammetry which were explained in previous sections, close range photogrammetry can be used for implementation of the data acquisition section in the system.

3.2 Reference surface reconstruction and parameterization (RSRP) section

Close range photogrammetry provides explicit 3D points measured around desired location on the body. For automatic diagnosing diseases using the points, it is necessary to define the normal pattern of the surface around the site. With access to such a surface, the system can use it as a reference surface in comparison with each other surfaces. The result of the comparison can be used as an indicator for disease diagnosing. For recognizing the normal pattern of the site surface, two problems should be considered. They are surface fitting and surface parameterization.

Fig. 5 Sample images**Table 3** Part of the list includes the output of data acquisition section

No.	X	Y	Z
1	67.5071	-42.8706	-234.6930
2	44.3282	-43.2111	-234.7885
3	37.3649	-68.0754	-196.3339
4	27.4084	-61.7780	-205.9730
5	24.0285	-74.2345	-186.5661
6	17.6009	-55.7681	-215.6088

**Fig. 6** SOM network architecture used in the case study

For fitting an appropriate surface to the points, its parameters should be known, and for parameterization process, shape of the surface should be recognized. There are different parameterization methods which cause generating surfaces with different characteristics. An appropriate parameterization method should satisfy four conditions [22]: neighborhood preservation, boundary interpolation, non-self-intersection, and uniform parametric

density. After parameterization process, fitting surface should be carried out in a way that the surface fulfills conditions such as shape preservation, smoothness, and accuracy. According to the mentioned needs and the advantages of SOM, in the system designed and implemented in this research, SOM technique has been used to parameterize and fit the surface simultaneously.

Input of this section is a dataset including 3D coordinates of the points measured on the body of healthy people. The dataset is provided by data acquisition section using the images acquired from body of several healthy individuals, and all are used to create reference surface by SOM simultaneously. Increasing the number of healthy subjects participated in the sampling process increases the reliability of the reference surface. The output of this section is stored as a functional surface with determined parameters and topology.

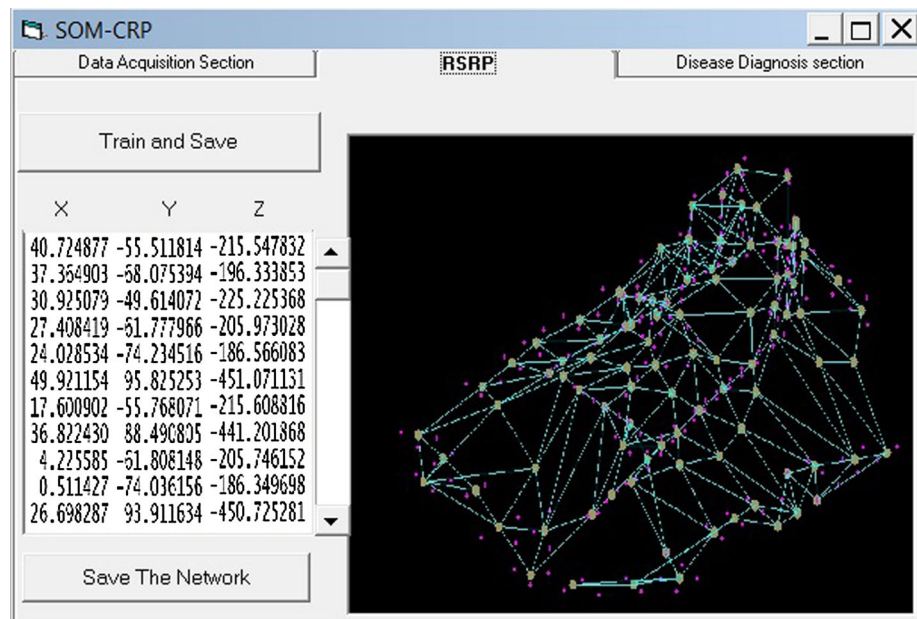
3.3 Disease diagnosis section

This section has two inputs:

1. Three-dimensional coordinates of the points measured around desired location on the body of a clinically affected person. They are provided by data acquisition section.
2. The reference surface provided by RSRP section

For diagnosing a disease, the set of 3D coordinates of the measured points is entered to the function of the reference surface, and the evaluation algorithm of SOM is used to determine the consistency of the dataset with the

Fig. 7 SOM network topology after training process



pattern of the reference surface. The evaluation error exceeds the defined threshold, indicating that the measured points are not consistent with the pattern of the reference surface which shows a healthy surface. The flowchart of the process is shown in Fig. 1.

The system architecture is shown in Fig. 2.

4 System implementation and evaluation

All algorithms and sections of the system have been implemented using Visual Basic programming language. The user interface of the system is shown in Fig. 3.

For evaluation of the system performance, in a case study, the system was trained and used for diagnosing foot deformity. Different steps of the case study have been explained in this section.

In the case study, a nonmetric digital camera was used to capture the images needed for data acquisition section. Specifications of the camera have been shown in Table 1. For calibration of the camera, 12 convergent images (4 of them by $+90^\circ$ rotation and 4 by -90°) captured from a portable target sheet (Fig. 4) were used in bundle adjustment process. The result of camera calibration is shown in Table 2. One unhealthy and five healthy persons were selected as samples for collecting training and test data, and following steps were carried out for all of them.

For measuring 3D coordinates of the key areas of foot (around heel, forefoot and arc), the areas were targeted using circles with 2 mm diameter. Also, a scale bar and some coded targets were installed around the foot. Six

positions were considered for imaging in a way that the angle between sight lines from two adjacent stations became about 60° and maximum distance between camera and the subject became 50 cm. Two sample images are shown in Fig. 5.

In data acquisition section, bundle adjustment method was used to calculate 3D coordinates of the selected points. For each person, the calculated coordinates of 100 selected points were stored in a list as the output of data acquisition section. Table 3 shows a part of the lists.

In this case study, training dataset was obtained by integrating data of four lists from the five lists related to the healthy persons. This dataset was used to generate the reference surface and recognize the normal foot pattern in training process of SOM network. Since each of the lists included 3D coordinates of 100 points, the size of SOM network was set 10 by 10 (a network with 100 neurons). In the system, each neuron of the network should fit to a key point (the point which is selected to acquire sample data) location after training process. In the case study, 100 locations have been marked as key points. So, increasing the number of neurons has no effect on the accuracy of the system, but decreasing the number of neurons can cause decreasing the accuracy of the network. The network architecture has been shown in Fig. 6. After 340 iterations, the network became stable. Figure 7 shows the network topology after training process.

For evaluation of the system performance, two remaining datasets, one belonging to the healthy person and another belonging to the unhealthy person, were entered to disease diagnosis section. The data belonging to healthy

Fig. 8 Performance of disease diagnosis section on the dataset belonging to the unhealthy person

NO	X	Y	Z	NO	Residual(mm)
54	-76.6351	42.6378	-369.1545	54	2.7
55	-79.3101	30.6801	-349.5999	55	3.7
56	-115.2255	23.9633	-338.5762	56	10.1
57	94.1957	-30.4923	-253.8112	57	10.4
58	104.0726	-37.0614	-244.3202	58	5.7
59	138.1811	71.3932	-415.5296	59	6.1
60	38.7501	43.6975	-276.1624	60	2.1
61	-2.8795	64.7666	-323.2361	61	5.7

RMSE= 7.3 mm

person was fitted to the reference surface with a root-mean-square error (RMSE) of 1.4 mm, but the process of matching the dataset belonging to the unhealthy person was failed with a RMSE of 7.3 mm, and the system identified the unhealthy person correctly (Fig. 8).

5 Conclusion

Close range photogrammetry is a technique which can accurately measure 3D coordinates of points on a desired object. The output of close range photogrammetry is a point cloud with no topology and structure. For diagnostic applications, the spatial pattern of the points must be recognized and a surface with definable topology must be fitted to them. The research result shows that SOM is an effective tool for recognizing the pattern of measured points and generating the reference surface. So, close range photogrammetry and SOM can be used to develop integrated systems as two complementary techniques.

In the research, SOM and close range photogrammetry have been employed for automatic diagnosing foot deformity. Using the architecture of the system for diagnosing other diseases whose symptoms are visible or appear as deformations out of body is suggested for future studies.

In the system introduced in the paper, 3D points measured via close range photogrammetry are used for constructing the required 3D model. Three-dimensional points which their coordinates are measured via other measurement techniques can be used as input data for the system. So, other researchers can apply SOM as a tool for

constructing 3D models in the application which their measurement techniques are not photogrammetry.

References

- Atkinson KB (2001) Close range photogrammetry and machine vision. Whittles Publishing, Scotland
- Mitchell HL, Newton I (2002) Medical photogrammetric measurement: overview and prospects. *ISPRS J Photogramm Remote Sens* 56(5–6):286–294
- Majid Z et al (2005) Photogrammetry and 3D laser scanning as spatial data capture techniques for a national craniofacial database. *Photogram Rec* 20(109):48–68
- Remondino F (2004) 3-D reconstruction of static human body shape from image sequence. *Comput Vis Image Underst* 93(1):65–85
- Normando D, Lima da Silva P, Mendes ÁM (2011) A clinical photogrammetric method to measure dental arch dimensions and mesio-distal tooth size. *Eur J Orthod* 33(6):721–726
- Boersma SM et al (2000) Photogrammetric wound measurement with a three-camera vision system. *ISPRS, Amsterdam*
- Farnood Ahmadi F, Layegh NF (2014) Integration of close range photogrammetry and expert system capabilities in order to design and implement optical image based measurement systems for intelligent diagnosing disease. *Measurement* 51:9–17
- Wen-Chang C (2006) Neural-network-based photometric stereo for 3D surface reconstruction. In: *International joint conference on neural networks. IJCNN '06*
- Lin W-C, Chen S-Y, Chen C-T (1989) A new surface interpolation technique for reconstructing 3D objects from serial cross-sections. *Comput Vis Gr Image Process* 48(1):124–143
- Xu M, Tang Z, Deng J (1995) A B-spline surface interpolation technique for reconstructing 3d objects from serial arbitrary shaped planar contours. In: *Chin R et al (eds) Image analysis applications and computer graphics. Springer, Berlin*, pp 74–82
- Kellman PJ, Garrigan P, Palmer EM (2011) 3D and spatiotemporal interpolation in object and surface formation. In: *Tyler CW*

- (ed) Computer vision: from surfaces to 3D objects, in computer vision: from surfaces to 3D objects. CRC Press, Taylor & Francis Group, New York, pp 183–207
12. Chia-Wei L, Medioni G (1994) Surface approximation of a cloud of 3D points. In: Proceedings of the 1994 2nd CAD-based vision workshop
 13. Park H, Kim K (1995) An adaptive method for smooth surface approximation to scattered 3D points. *Comput Aided Des* 27(12):929–939
 14. Nior ADMBJ, Neto AODDR, Melo JDD (2004) A self-organized neural network for 3D surface reconstruction. In: WSEAS, Italy
 15. Kohonen T (2011) Self-organizing maps, 3rd edn. Springer, New York
 16. Chong AK (2009) New developments in medical photogrammetr. *Geoinf Sci J* 9(1):41–50
 17. Tokarczyk R, Mazur T (2006) Photogrammetry—principles of operation and application in rehabilitation. *Med Rehabil* 10(4):30–39
 18. Sechidis L, Tsioukas V, Patias P (2000) An Automatic process for the extraction of the 3D model of the human back surface for scoliosis treatment. In: International archives of photogrammetry and remote sensing, Amsterdam
 19. D’apuzzo N, Mitchell H (2008) Medical applications. Table of contents for advances in photogrammetry, remote sensing, and spatial information: 2008 ISPRS congress book 2008. CRC Press, New York
 20. Kohonen T et al (1996) Engineering applications of the self-organizing map. *Proc IEEE* 84(10):1358–1384
 21. Self organizing maps—applications and novel algorithm design: InTech. 702
 22. Barhak J, Fischer A (2002) Adaptive reconstruction of freeform objects with 3D SOM neural network grids. *Comput Graph* 26(5):745–751